Synthesis and Evaluation of 5-Fluoro-2-aryloxazolo[5,4-b]pyridines as β-Amyloid PET Ligands and Identification of MK-3328

Scott T. Harrison,*,[†] James Mulhearn,[†] Scott E. Wolkenberg,[†] Patricia J. Miller,[‡] Stacey S. O'Malley,[‡] Zhizhen Zeng,[‡] David L. Williams, Jr.,[‡] Eric D. Hostetler,[‡] Sandra Sanabria-Bohórquez,[‡] Linda Gammage,[‡] Hong Fan,[‡] Cyrille Sur,[‡] J. Christopher Culberson,[§] Richard J. Hargreaves,[‡] Jacquelynn J. Cook,[‡] George D. Hartman,[†] and James C. Barrow[†]

[†]Departments of Medicinal Chemistry, [‡]Imaging, and [§]Chemical Modeling and Informatics, Merck Research Laboratories, Merck & Co., Inc., P.O. Box 4, West Point, Pennsylvania 19486, United States

S *Supporting Information*

ABSTRACT: 5-Fluoro-2-aryloxazolo[5,4-b]pyridines were synthesized and investigated as potential ^{18}F containing β-amyloid PET ligands. In competition binding assays using human AD brain homogenates, compounds **14b**, **16b**, and **17b** were identified as having favorable potency versus human β-amyloid plaque and were radiolabeled for further evaluation in *in vitro* binding and *in vivo* PET imaging experiments. These studies led to the identification of **17b** (MK-3328) as a candidate PET ligand for the clinical assessment of β-amyloid plaque load.

KEYWORDS: Alzheimer's disease, β-amyloid plaque, fluorine-18, positron emission tomography, PET, oxazolo[5,4-b]pyridine
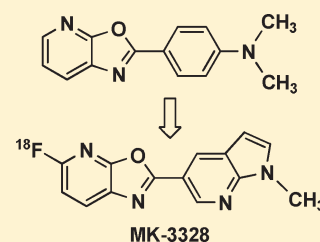
Alzheimer's disease (AD) is a progressive neurodegenerative disorder which was estimated to afflict 26.6 million people worldwide as of 2006,[1] with many more being affected as caregivers of those with this debilitating disease. Although marketed treatments for AD temporarily improve cognitive symptoms in patients, they fail to significantly slow disease progression. Several novel therapeutics are under development which have the potential to intervene in the underlying mechanisms of AD, and biomarkers for detecting affected patient populations and for measuring response to these therapies are needed.[2] Many in the Alzheimer's research community believe that successful alteration of the disease's trajectory may require therapeutic intervention at the mild cognitive impairment (MCI) symptomatic stage, before the onset of potentially irreversible neurodegeneration.[3] Whereas clinical diagnosis of AD via tests of cognition is sufficient at late stages, early diagnosis of prodromal or predementia AD is less straightforward and requires evidence of both episodic memory loss and biomarker changes supportive of pathological processes.[4]

Several noteworthy efforts are underway to identify early clinical markers of AD.[5] While promising, most predictive markers are indirect measures of underlying disease pathology or are medically invasive. A more direct and noninvasive approach, in particular, the assessment of β-amyloid (Aβ) plaque deposits in the brain via positron emission tomography (PET) imaging, has demonstrated success in clinical settings. To date, several Aβ-binding PET ligands have effectively differentiated AD from non-AD patients. [^{11}C]PIB (**1**, Figure 1)[6,7] is the most thoroughly studied amyloid PET ligand and recently has been correlated with other clinical AD biomarkers.[8] Although not as well characterized as PIB, Astra-Zeneca's [^{11}C]AZD2184 (**2**) shows promise as a human amyloid imaging agent, as it has
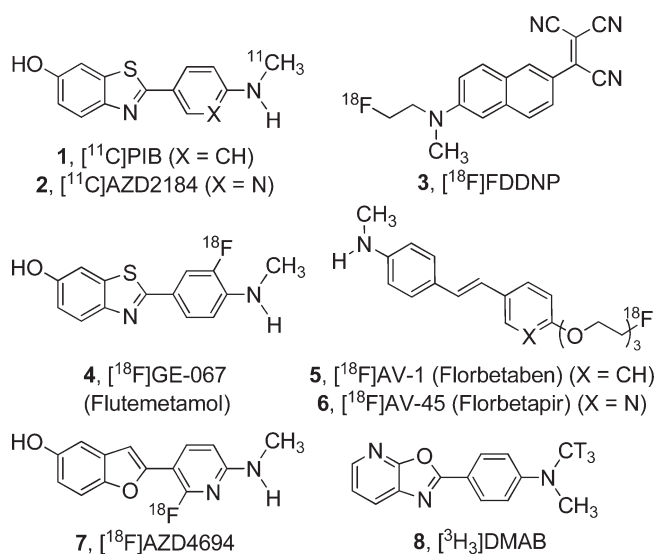

**Figure 1.** Structures of selected amyloid PET ligands and our reference radioligand **8**, [^{3}H$_3$]DMAB.

demonstrated lower levels of nonspecific binding than PIB in preclinical studies.[9−11]

While these tracers are effective, the short half-life of ^{11}C (∼20 min) limits the use of [^{11}C]PIB and [^{11}C]AZD2184 to PET imaging centers with cyclotrons in their immediate vicinity.

Scheme 1[a]
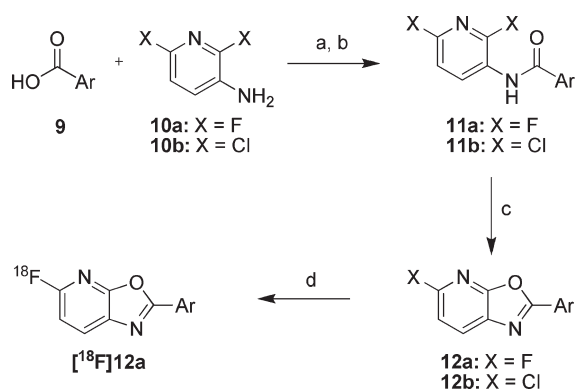
[a] Reagents and conditions: (a) 9, $(CH_3)_2C=C(N(CH_3)_2)Cl$, CH_2Cl_2, 25 °C. (b) 10a or 10b, pyridine, 25 °C. (c) K_2CO_3 or Cs_2CO_3, DMF, microwave, 165 °C; optionally TFA, 25 °C. (d) $K^{18}F$, kryptofix 2.2.2, DMSO, microwave, 140 °C, 3 min. TFA = trifluoroacetic acid.

Because ^{18}F has a much longer half-life (110 min), ^{18}F-based tracers may be used at PET imaging sites much further away from radionuclide production sites, enabling increased access for patients. Several research programs have engaged in the design and discovery of ^{18}F amyloid PET ligands, culminating in the discovery of $[^{18}F]FDDNP[12]$ (3), GE-067 (Flutemetamol, 4),[13] $[^{18}F]AV-1$ (Florbetaben, 5),[14,15] $[^{18}F]AV-45$ (Florbetapir, 6),[16,17] and AZD4694 (7).[18]

Based on the preclinical and clinical data available,[12−18] we estimated that a successful amyloid imaging agent must have high affinity for β-amyloid plaque (K_d < 20 nM) with minimal nonspecific binding in order to provide a large specific signal for plaque detection. Also important is the behavior of the tracer in *in vivo* imaging studies in animals lacking plaque, where the tracer should exhibit high brain uptake and rapid washout kinetics. Published data on amyloid ligand candidates reveals that highly lipophilic tracers often exhibit elevated retention in white matter which, in imaging studies, can affect the signal-to-noise ratio and interfere with the differentiation of AD and non-AD patients.[15] Decreasing lipophilicity (e.g., cLogP) is one method that may be employed to reduce nonspecific binding to brain tissue.[19] Pairwise comparisons of closely related amyloid binders suggests that this approach is valid, as observed in the improved nonspecific binding profile of AZD2184 (cLogP[20] = 2.84) versus PIB (cLogP = 3.45) as well as AV-45 (cLogP = 3.13) versus AV-1 (cLogP = 3.75).

Herein we report our efforts in this area, involving the synthesis and evaluation of oxazolo[5,4-b]pyridines that can be labeled with ^{18}F as potential imaging agents for β-amyloid plaque. To characterize binding of newly synthesized compounds, a competition binding assay in human AD cortex homogenates was employed using $[^3H_3]DMAB$ (8) as a reference radioligand. This compound was identified via radiolabeling of selected structures from the Merck compound collection with high structural similarity to literature amyloid plaque ligands. $[^3H_3]DMAB$ (8) has a K_d of 25 nM in human AD brain homogenates with low levels of nonspecific binding, making it a suitable reference radioligand for competition binding assays. From a design perspective, 8 also served as a lead structure in the design of the 5-fluoro-oxazolo[5,4-b]pyridines presented in this work. Potent compounds possessing low calculated logP and lacking P-glycoprotein (P-gp) susceptibility were radiolabeled

Table 1. Affinity of 5-Fluoro-2-aryloxazolo[5,4-b]pyridines for Human β-Amyloid Plaque Deposits

Compound	Ar	Aβ IC$_{50}$ (nM)[a]	cLogP[b]
13		32.5	3.11
14a: R = H		23.1	2.59
14b: R = CH$_3$		4.0	2.94
15a: R = H		102	1.97
15b: R = CH$_3$		41.8	2.33
16a: R = H		13.8	3.07
16b: R = CH$_3$		8.0	3.28
17a: R = H		25.7	1.98
17b: R = CH$_3$		10.5	2.18
18		47.0	2.40
19		30.2	1.53
20		35.8	3.21
21		45.3	3.07
22		48.7	2.63
23		>1000	2.55
24		>1000	2.50

[a] Values are means of at least two experiments. [b] Calculated using AlogP98.[20]

with tritium for examination in more detailed *in vitro* binding assays and with ^{18}F for evaluation in rhesus monkey PET studies. Because $[^{11}C]PIB$ does not bind with high affinity to plaque in rhesus monkey brain,[21] we did not use animal models of AD in *in vivo* imaging experiments to predict the behavior of tracer candidates in patients.

Unlabeled oxazolo[5,4-b]pyridine analogs were synthesized starting from 3-amino-2,6-difluoropyridine 10a[22] (Scheme 1) and a variety of commercially available and prepared carboxylic acids 9. Activation of the carboxylic acids 9 with Ghosez' reagent,[23] followed by reaction with 10a in the presence of excess pyridine afforded amides of type 11a. Focused libraries were prepared by parallel concentration of the crude reaction mixtures and direct passage into the next step; however, conversions were generally higher if the amides were first isolated and

Table 2. Binding Affinity of Tritium-Labeled 14b, 16b, and 17b versus Human AD Brain Homogenates from Three Different Donors

compd	K_d (nM)[a]	B_{max} (nM)	B_{max}/K_d	NDB[b]
[^{3}H$_3$]14b	4.5 ± 0.6	2088 ± 231	464 ± 80	50%
[^{3}H$_3$]16b	6.4 ± 0.9	1454 ± 140	232 ± 40	50%
[^{3}H$_3$]17b	9.6 ± 0.3	1100 ± 290	117 ± 34	35%

[a] Values are means of three experiments using AD brain homogenates from different donors. [b] Nondisplaceable binding, estimated as the amount of binding observed at the K_d in the presence of 2 μM unlabeled compound

purified, using either chromatography or precipitation following the addition of water. Previously described acidic methods for the conversion of amides of type **11a** into oxazolo[5,4-*b*]pyridines were poor yielding;[24] however, microwave heating of the amides **11a** with K_2CO_3 or Cs_2CO_3 in DMF afforded the targeted oxazolo[5,4-*b*]pyridines **12a**, typically with high conversion. In instances where the starting carboxylate **9** contained a free N—H, the base mediated cyclizations failed to proceed, necessitating protection with a Boc or *p*-methoxybenzyl group, which either spontaneously deprotected during heating or was subsequently removed with trifluoroacetic acid. Synthesis of ^{18}F labeled precursors was accomplished via the same route, substituting commercially available 3-amino-2,6-dichloropyridine **10b** in the first step, leading to 5-chloro-oxazolo[5,4-*b*]pyridines of type **12b**. Microwave heating with [^{18}F]KF and Kryptofix 2.2.2 in DMSO then afforded [^{18}F]**12a**.

Previously reported SAR in the 2-arylbenzazole classes of Aβ plaque ligands suggested that 4- and 3,4-substitutions on the 2-aryl ring are necessary for high amyloid affinity,[25] while 2- and 6-substitutions are deleterious, so our own efforts primarily focused on the 3- and 4-positions (Table 1). While 4-methoxyphenyl (**13**) and 4-methylaminophenyl (**14a**) analogs demonstrated moderate potency with moderate to high clogP values, the dimethylamino analog **14b** exhibited potent binding, with only a slightly higher clogP relative to **14a**. Attempts to moderate lipophilicity by incorporation of a ring nitrogen, as in pyridine analogs **15a** and **15b**, resulted in a loss of binding affinity. Constraining the 4-substituent into a ring led to indole analogs **16a** and **16b**, which were potent at a cost of slightly elevated lipophilicity. Whereas aza-substitution of 4-amino phenyl compounds was deleterious for binding potency, 7-aza-substitution of the indoles **16a**–**b**, affording the azaindoles **17a** and **17b**, caused only a 2-fold loss in binding potency while lowering clogP by a full unit. *N*-Methyl analogs (**14b**–**17b**) tended to exhibit improved binding potency relative to their respective *des*-methyl analogs (**14a**–**17a**). Many closely related and isomeric forms of the active indoles (**16a,b**) and azaindoles (**17a,b**) were investigated; however, the best of these compounds were 2- to 5-fold less potent (**18**–**22**) and, in most instances, were completely inactive (e.g., **23**–**24**). All of the compounds evaluated for human P-gp susceptibility in this series were not substrates (P-gp transport ratio < 3) and exhibited high passive permeability ($P_{app} > 20 \times 10^{-6}$ cm/s), including the lead compounds **14b**, **16b**, and **17b**.[26]

To fully characterize the binding characteristics of **14b**, **16b**, and **17b**, their corresponding [^{3}H$_3$]methyl analogs were prepared using sodium hydride mediated deprotonation of **14a**, **16a**, and **17a**, respectively, followed by reaction with [^{3}H$_3$]methyl
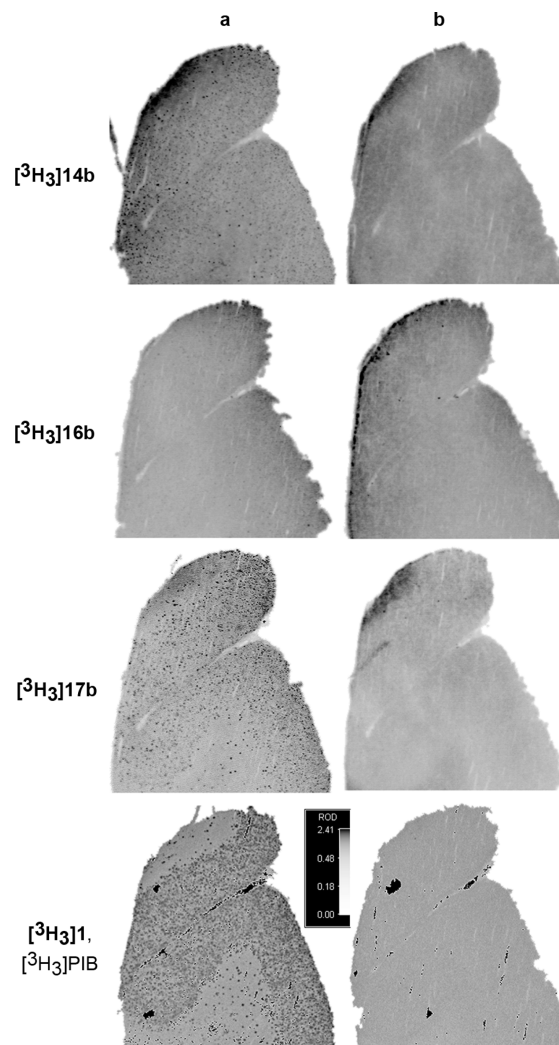

Figure 2. (a) Autoradiographic images of AD human cortex after treatment with 5 nM [^{3}H$_3$]-labeled compound. (b) Autoradiographic images of AD human cortex after treatment with 5 nM [^{3}H$_3$]-labeled compound in the presence of 1 μM unlabeled compound (self-block).

iodide. Saturation binding studies were conducted using AD cortex homogenates, to which all three compounds exhibited potent and saturable binding (Table 2). While **14b** and **16b** exhibited more potent binding and higher B_{max}/K_d ratios relative to **17b**, the latter compound exhibited lower levels of nondisplacable binding in AD brain homogenates, estimated as the percent of total binding at the K_d in the presence of 2 μM unlabeled compound. The decreased level of nonspecific binding associated with **17b** is consistent with the hypothesis that nonspecific binding to brain tissue correlates with lipophilicity.

Autoradiographic imaging experiments with human AD brain slices were used to further differentiate the tritium-labeled lead compounds (Figure 2). Whereas [^{3}H$_3$]**14b**, [^{3}H$_3$]**17b**, and the positive control [^{3}H$_3$]PIB ([^{3}H$_3$]**1**)[9] exhibited a punctate binding pattern, [^{3}H$_3$]**16b** repeatedly failed to do so, presumably due to a combination of elevated nonspecific binding and a high affinity of the compound for laboratory plastics (Figure 2, column a). Self-block with 1 μM unlabeled parent compound was used to assess nonspecific binding (Figure 2, column b). In all instances, punctate binding was not observed in the presence
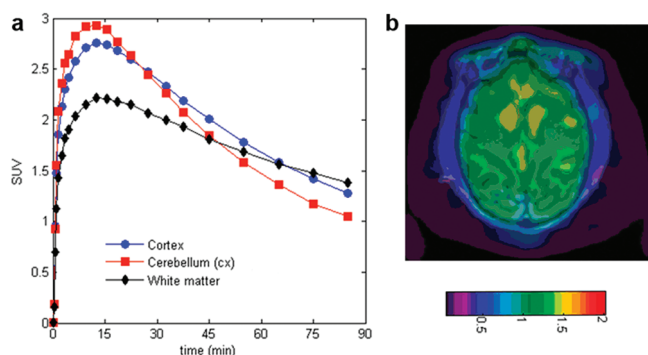
500

dx.doi.org/10.1021/ml200018n |*ACS Med. Chem. Lett.* 2011, 2, 498–502

Figure 3. (a) Decay corrected time−activity curves for [^{18}F]**17b** in cortex (red circles), cerebellum (blue squares), and white-matter (black diamonds). (b) MRI coregistered rhesus PET image at 45−90 min with [^{18}F]**17b**. Cerebellum was used as a baseline reference.

of a saturating concentration of unlabeled parent compound; however, all compounds exhibited some degree of diffuse background binding. Qualitatively, the specific to nonspecific binding ratio for [^{3}H$_{3}$]**17b** appeared to be better than that of [^{3}H$_{3}$]**14b**, suggesting that **17b** may be a better amyloid diagnostic agent *in vivo*.

Using the chemistry delineated in Scheme 1, ^{18}F-labeled versions of **14b**, **16b**, and **17b** were prepared for evaluation in *in vivo* PET imaging studies in healthy anesthetized rhesus monkeys to evaluate brain uptake and washout kinetics, and the preliminary data for [^{18}F]**17b** is depicted in Figure 3.[27] Here the tracer demonstrated high peak brain uptake of ca. 2.7 standardized uptake value (SUV) units in cortex and ca. 3.0 SUV in the cerebellum. As desired, [^{18}F]**17** washed out rapidly, with less than half of the peak uptake present in the cortex and cerebellum at 90 min. In humans exhibiting AD pathology, amyloid plaque deposits manifest themselves throughout the brain, including the cortex, but not in the cerebellum until terminal phases of the disease.[28] The close correlation between cerebellum and cortex time activity curves in this study is desirable, as it suggests that the cerebellum will likely be a suitable baseline reference region in clinical imaging studies. In the 45−90 min summed image (Figure 3b), cortical regions show a lack of hot spots corresponding to white matter retention. Preliminarily, this may suggest that the approach of minimizing white matter binding via targeting of less lipophilic amyloid ligands is valid. Whether or not this lack of white matter retention in rhesus will translate into human clinical imaging is a matter of future study.

In conclusion, we have investigated 5-fluoro-2-aryloxazolo-[5,4-*b*]pyridines as potential β-amyloid PET ligands. After screening newly synthesized compounds for affinity toward AD brain homogenates, **17b** (MK-3328) was identified as a promising candidate, exhibiting amyloid binding potency balanced with low levels of nonspecific binding. *In vivo*, [^{18}F]**17b** demonstrates favorable kinetics, exhibiting high brain uptake and good washout in normal rhesus monkey PET imaging studies. Human clinical trials to evaluate [^{18}F]MK-3328 as an ^{18}F-based β-amyloid PET ligand are currently underway and will be reported upon in due course.

ASSOCIATED CONTENT

Ⓢ **Supporting Information.** Representative assay and experimental procedures and characterization data for tested compounds. This material is available free of charge via the Internet at http://pubs.acs.org.

AUTHOR INFORMATION

Corresponding Author
*Telephone: +1-215-652-7652. Fax: +1-215-652-6345. E-mail: scott_harrison@merck.com.

ACKNOWLEDGMENT

REFERENCES

(1) Brookmeyer, R.; Johnson, E.; Ziegler-Graham, K.; Arrighi, H. M. Forecasting the global burden of Alzheimer's disease. *Alzhimer's Dementia* **2007**, *3*, 186–191.

(2) Galimberti, D.; Scarpini, E. Treatment of Alzheimer's Disease: Symptomatic and Disease-Modifying Approaches. *Curr. Aging Sci.* **2010**, *3*, 46–56.

(3) Peterson, R. C.; Roberts, R. O.; Knopman, D. S.; Boeve, B. F.; Geda, Y. E.; Ivnik, R. J.; Smith, G. E.; Jack, C. R., Jr. Mild Cognitive Impairment. *Arch. Neurol.* **2009**, *66*, 1447–1455.

(4) Dubois, B.; Feldman, H. H.; Jacova, C.; Cummings, J. L.; DeKosky, S. T.; Barberger-Gateau, P.; Delacourte, A.; Frisoni, G.; Fox, N. C.; Galasko, D.; Gauthier, S.; Hampel, H.; Jicha, G. A.; Meguro, K.; O'Brien, J.; Pasquier, F.; Robert, P.; Rossor, M.; Salloway, S.; Sarazin, M.; de Souza, L. C.; Stern, Y.; Visser, P. J.; Scheltens, P. Revising the definition of Alzheimer's disease: a new lexicon. *Lancet Neurol.* **2010**, *9*, 1118–1127.

(5) Blennow, K.; Hampel, H.; Weiner, M.; Zetterberg, H. Cerebrospinal fluid and plasma biomarkers in Alzheimer disease. *Nature Rev. Neurol.* **2010**, *6*, 131–144.

(6) Mathis, C. A.; Wang, Y.; Holt, D. P.; Huang, G.-F.; Debnath, M. L.; Klunk, W. E. Synthesis and Evaluation of ^{11}C-Labeled 6-Substituted 2-Arylbenzothiazoles as Amyloid Imaging Agents. *J. Med. Chem.* **2003**, *46*, 2740–2754.

(7) Klunk, W. E.; Engler, H.; Nordberg, A.; Wang, Y.; Blomqvist, G.; Holt, D. P.; Bergström, M.; Savitcheva, I.; Huang, G.-F.; Estrada, S.; Ausen, B.; Debnath, M. L.; Barletta, J.; Price, J. C.; Sandell, J.; Lopresti, B. J.; Wall, A.; Koivisto, P.; Antoni, G.; Mathis, C. A.; Långström, B. Imaging brain amyloid in Alzheimer's disease with Pittsburgh Compound-B. *Ann. Neurol.* **2004**, *55*, 306–319.

(8) Degerman, G. M.; Lindau, M.; Wall, A.; Blennow, K.; Darreh-Shori, T.; Basu, S.; Nordberg, A.; Larsson, A.; Lannfelt, L.; Basun, H.; Kilander, L. Pittsburgh compound-B and Alzheimer's disease biomarkers in CSF, plasma and urine: An exploratory study. *Dementia Geriatr. Cognit. Disord.* **2010**, *29*, 204–212.

(9) Swahn, B.-M.; Wensbo, D.; Sandell, J.; Sohn, D.; Slivo, C.; Pyring, D.; Malmström, J.; Arzel, E.; Vallin, M.; Bergh, M.; Jeppsson, F.; Johnson, A. E.; Juréus, A.; Neelissen, J.; Svensson, S. Synthesis and evaluation of 2-pyridylbenzothiazole, 2-pyridylbenzoxazole and 2-pyridylbenzofuran derivatives as ^{11}C-PET imaging agents for β-amyloid plaques. *Bioorg. Med. Chem. Lett.* **2010**, *20*, 1976–1980.

(10) Johnson, A. E.; Jeppsson, F.; Sandell, J.; Wensbo, D.; Neelissen, J. A. M.; Jureus, A.; Stroem, P.; Norman, H.; Farde, L.; Svensson, S. P. S. AZD2184: a radioligand for sensitive detection of β-amyloid deposits. *J. Neurochem.* **2009**, *108*, 1177–1186.

(11) Svante, N.; Eriksdotter, J. M.; Zsolt, C.; Christer, H.; Per, J.; Hans, O.; Yvonne, F.-L.; Jan, A.; Katarina, V.; Samuel, S.; Lars, F. Detection of amyloid in Alzheimer's disease with positron emission

501

dx.doi.org/10.1021/ml200018n |*ACS Med. Chem. Lett.* 2011, 2, 498–502

tomography using [^{11}C]AZD2184. *Eur. J. Nucl. Med. Mol. Imaging* **2009**, *36*, 1859–1863.

(12) Small, G. W.; Kepe, V.; Ercoli, L.; Siddarth, P.; Bookheimer, S. Y.; Miller, K. J.; Lavretsky, H.; Burggren, A. C.; Cole, G. M.; Vinters, H. V.; Thompson, P. M.; Huang, S.-C.; Satyamurthy, N.; Phelps, M. E.; Barrio, J. R. PET of brain amyloid and tau in mild cognitive impairment. *N. Engl. J. Med.* **2006**, *355*, 2652–2663.

(13) Vandenberghe, R.; Van Laere, K.; Ivanoiu, A.; Salmon, E.; Bastin, C.; Triau, E.; Hasselbalch, S.; Law, I.; Andersen, A.; Korner, A.; Minthon, L.; Garraux, G.; Nelissen, N.; Bormans, G.; Buckley, C.; Owenius, R.; Thurfjell, L.; Farrar, G.; Brooks, D. J. ^{18}F-flutemetamol amyloid imaging in Alzheimer disease and mild cognitive impairment: a phase 2 trial. *Ann. Neurol.* **2010**, *68*, 319–329.

(14) Zhang, W.; Oya, S.; Kung, M. P.; Hou, C.; Maier, D. L.; Kung, H. F. F-18 PEG stilbenes as PET imaging agents targeting Aβ aggregates in the brain. *Nucl. Med. Biol.* **2005**, *32*, 799–809.

(15) Rowe, C. C.; Ackerman, U.; Browne, W.; Mulligan, R.; Pike, K. L.; O'Keefe, G.; Tochon-Danguy, H.; Chan, G.; Berlangieri, S. U.; Jones, G.; Dickinson-Rowe, K. L.; Kung, H. P.; Zhang, W.; Kung, M. P.; Skovronsky, D.; Dyrks, T.; Holl, G.; Krause, S.; Friebe, M.; Lehman, L.; Lindemann, S.; Dinkelborg, L. M.; Masters, C. L.; Villemagne, V. L. Imaging of amyloid β in Alzheimer's disease with ^{18}F-BAY94-9172, a novel PET tracer: proof of mechanism. *Lancet Neurol.* **2008**, *7*, 129–135.

(16) Zhang, W.; Kung, M. P.; Oya, S.; Hou, C.; Kung, H. F. ^{18}F-Labeled styrylpyridines as PET agents for amyloid plaque imaging. *Nucl. Med. Biol.* **2007**, *34*, 89–97.

(17) Wong, D. F.; Rosenberg, P. B.; Zhou, Y.; Kumar, A.; Raymont, V.; Ravert, H. T.; Dannals, R. F.; Nandi, A.; Brasić, J. R.; Ye, W.; Hilton, J.; Lyketsos, C.; Kung, H. F.; Joshi, A. D.; Skovronsky, D. M.; Pontecorvo, M. J. In Vivo Imaging of Amyloid Deposition in Alzheimer Disease Using the Radioligand ^{18}F-AV-45 (Flobetapir F 18). *J. Nucl. Med.* **2010**, *51*, 913–920.

(18) Juréus, A.; Swahn, B.-M.; Sandell, J.; Jeppsson, F.; Johnson, A. E.; Johnström, P.; Neelissen, J. A. M.; Sunnemark, D.; Farde, L.; Svensson, S. P. S. Characterization of AZD4694, a novel fluorinated Aβ plaque neuroimaging PET radioligand. *J. Neurochem.* **2010**, *114*, 784–794.

(19) Summerfield, S. G.; Read, K.; Begley, D. J.; Obradovic, T.; Hidalgo, I. J.; Coggon, S.; Lewis, A. V.; Porter, R. A.; Jeffrey, P. Central Nervous System Drug Disposition: The Relationship between in Situ Brain Permeability and Brain Free Fraction. *J. Pharmacol. Exp. Ther.* **2007**, *322*, 205–213.

(20) AlogP98 values were calculated by Cerius2 (version 4.11) from Accelrys (San Diego, CA).Ghose, A. K.; Viswanadhan, V. N.; Wendolowski, J. J. Prediction of Hydrophobic (Lipophilic) Properties of Small Organic Molecules Using Fragmental Methods: An Analysis of ALOGP and CLOGP Methods. *J. Phys. Chem. A* **1998**, *102A*, 3762–3772.

(21) Rosen, R. F.; Walker, L. C.; Levine, H., III. PIB binding in aged primate brain: Enrichment of high-affinity sites in humans with Alzheimer's disease. *Neurobiol. Aging* **2011**, *32*, 223–234.

(22) Radl, S.; Hradil, P. Synthesis of some 1-alkyl-1,4-dihydro-4-oxo-1,7-naphthyridine-3-carboxylic acids. *Collect. Czech. Chem. Commun.* **1991**, *56*, 2420–2429.

(23) Devos, A.; Remion, J.; Frisque-Hesbain, A. M.; Colens, A.; Ghosez, L. Synthesis of acyl halides under very mild conditions. *J. Chem. Soc., Chem. Commun.* **1979**, *24*, 1180–1181.

(24) Flouzat, C.; Guillaumet, G. A new convenient synthesis of 2-aryl- and 2-heteroaryloxazolo[5,4-b]pyridines. *Synthesis* **1990**, *1*, 64–66.

(25) Cai, L.; Innis, R. B.; Pike, V. W. Radioligand development for PET imaging of β-amyloid (Aβ)-current status. *Curr. Med. Chem.* **2007**, *14*, 19–52.

(26) Yamazaki, M.; Neway, W. E.; Ohe, T.; Chen, I. W.; Rowe, J. F.; Hochman, J. H.; Chiba, M.; Lin, J. H. In vitro substrate identification studies for P-glycoprotein mediated transport: species difference and predictability of in vivo results. *J. Pharmacol. Exp. Ther.* **2001**, *296*, 723–735.

(27) The detailed synthesis of [^{18}F]**14b**, [^{18}F]**16b**, and [^{18}F]**17b** and their comparison in *in vivo* rhesus PET imaging experiments is the subject of a separate communication: Hostetler, E. D.; Sanabria-Bohórquez, S.; Fan, H.; Zeng, Z.; Gammage, L.; Miller, P.; O'Malley, S.; Connolly, B.; Mulhearn, J.; Harrison, S. T.; Wolkenberg, S. E.; Barrow, J. C.; Williams, D. L., Jr.; Hargreaves, R. J.; Sur, C.; Cook, J. J. [^{18}F]Fluoroazabenzoxazoles as Potential Amyloid Plaque PET Tracers: Synthesis and *In Vivo* Evaluation in Rhesus Monkey. *Nucl. Med. Biol.*, in press.

(28) Thal, D. R.; Griffin, W. S. T.; Braak, H. Parenchymal and vascular Aβ-deposition and its effects on the degeneration of neurons and cognition in Alzheimer's disease. *J. Cell. Mol. Med.* **2008**, *12*, 1848–1862.